

Surface-activated Bonding of III-V Compound Semiconductors and Si for Fabricating Hybrid Tandem Solar Cells

Naoteru Shigekawa and Jianbo Liang

Graduate School of Engineering, Osaka City University, Osaka 558-8585, Japan

Abstract—The possibility of the surface-activated bonding (SAB) technologies for fabricating III-V-on-Si hybrid tandem solar cells is discussed. Although the electrical conduction across the bonding interfaces is influenced by the interface states introduced during the surface-activation process, their impacts are likely to be lowered by combining more heavily-doped bonding layers and the annealing process after the bonding. InGaP/GaAs/Si hybrid triple-junction cells are successfully fabricated by bonding III-V heterostructures for InGaP/GaAs double-junction cells and Si cell structures. This means that the bonding interfaces have an enough tolerance against the possible stress during the conventional device process sequence and that the SAB is promising as a practical substitute for the conventional semiconductor growth technologies in fabricating III-V-on-Si tandem cells.

Keywords—surface-activated bonding; tandem cells; InGaP/GaAs/Si; interface properties

I. INTRODUCTION

Among various kinds of structures for solar cells targeting high efficiencies, multi junction or tandem cells fabricated by stacking sub cells with different band gaps are most promising from the practical viewpoints [1], [2]. Specifically III-V-on-Si tandem cells, which are stacks of sub cells made of III-V compound semiconductors as wider band gap parts on Si-based bottom cells, are assumed to be one of the leading candidates for fulfilling requirements of both high efficiencies and low costs. In general, however, III-V heterostructures cannot be easily grown on Si substrates due to the difference in lattice constants and thermal expansion coefficients [3].

The surface-activated bonding (SAB) [4], [5] is likely to be a substitute for the heteroepitaxial growth of III-V layers on Si since using the SAB dissimilar semiconductor materials can be firmly bonded to each other without heating [6]. It is noteworthy, however, that the surfaces of semiconductor bonding layers could be damaged by the fast atom beams during the surface-activation process and the electrical conduction across the bonding interfaces might be influenced by the resultant interface states.

We have been exploring the possibility of SAB for fabricating InGaP/GaAs/Si hybrid triple-junction (3J) cells [7], [8]. We have also been investigating the electrical properties of bonding interfaces [9]–[12]. In this paper we summarize the results that we obtained and discuss the feasibility and remaining issues of the SAB technologies applied for fabricating hybrid tandem cells.

II. STRUCTURAL AND ELECTRICAL PROPERTIES OF BONDING INTERFACES

We fabricated n -Si/ n -Si and p -Si/ p -Si junctions and measured their current-voltage-temperature characteristics after

they were annealed at different temperatures. We analyzed the dependencies of the conductance at the zero-bias voltage on the ambient temperature by using the thermionic emission model and estimated the heights of barriers formed at the bonding interfaces. In the framework of the empirical charge-neutral-level model [13], we assumed that the electrical charges due to the interface states should be balanced with the charges in the depletion layers both at the n -Si/ n -Si and p -Si/ p -Si interfaces, as is schematically shown in Fig. 1(a). Then we extracted the density of interface states (D_{it}) for Si/Si interfaces annealed at the respective temperatures. The dependencies of the heights of barriers in n -Si/ n -Si and p -Si/ p -Si junctions and D_{it} on the annealing temperature are shown in Fig. 1(b). We found that D_{it} decreased as the annealing temperature increased [11]. Similar measurements and analyses were performed for GaAs/GaAs junctions [12], for which D_{it} also decreased with the increase of the annealing temperature.

Furthermore we performed XTEM observation of GaAs/Si junctions and confirmed that the amorphous-like layer, which had been apparent at the interface before being annealed, vanished due to the recrystallization during the annealing at 400 °C for 1 min [10]. The results that we obtained were similar to reports for Si/Si interfaces [5].

We measured current-voltage characteristics of heavily-doped pn junctions and estimated the resistance across the bonding interfaces. The relationship between the resistance and the effective concentration of impurities is shown in Fig. 2(a). We obtained lower resistances for interfaces with higher doping concentrations [9]. Figure 2(b) shows $I - V$ curves of n -GaAs/ n -Si junctions annealed at different temperatures after bonding. The lowest resistance was achieved in junctions annealed at the highest temperature (400 °C) as the inset of this figure shows [10]. The lower resistances for interfaces with more-heavily doped bonding layers was related to the abrupt change of their potential profiles. The dependence of the resistance on the annealing temperature is likely to be related to the re-crystallization of amorphous layers. The observed change in the resistance due to the annealing is promising results since such annealing process is essential for fabricating ohmic contacts on the emitters of III-V top cells.

III. FABRICATION AND CHARACTERIZATION OF INGaP/GAAS/SI TRIPLE-JUNCTION CELLS [7], [8]

III-V heterostructures for InGaP/GaAs double-junction cells with p -GaAs top (bonding) layers were prepared by MOCVD growth on GaAs substrates. Note that the heterostructures were

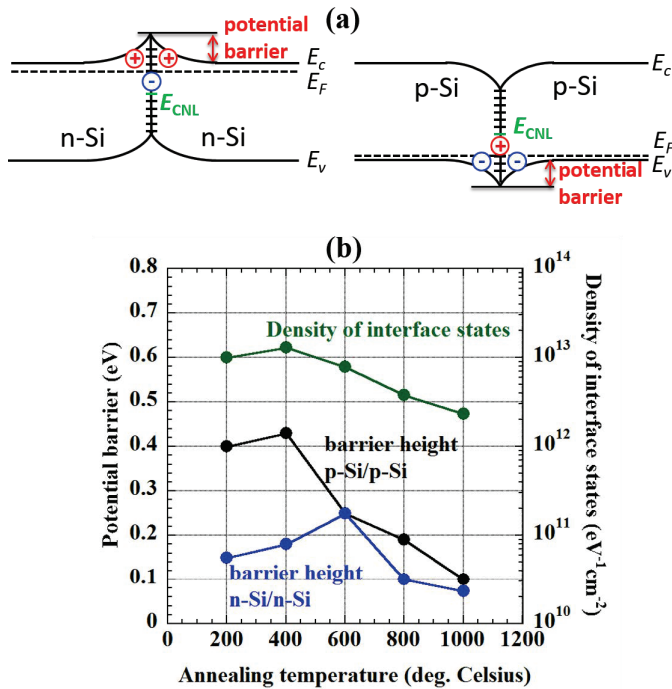


Fig. 1. (a) Schematic band diagrams of $n\text{-Si}/n\text{-Si}$ and $p\text{-Si}/p\text{-Si}$ junctions in the framework of charge neutral level model. Potential barriers are built at the interfaces so as to balance the charges in the depletion layers and those in the interface states. (b) The dependencies of the heights of barriers in $n\text{-Si}/n\text{-Si}$ and $p\text{-Si}/p\text{-Si}$ junctions and the density of interface states on the annealing temperature.

grown along the reverse direction. The heterostructures were bonded to $n\text{-on-p}$ Si cell structures that had been fabricated by the implantation of phosphor (P) and boron (B) ions and annealing. The InGaP/GaAs/Si 3J cells were fabricated by (i) selectively etching GaAs substrates, (ii) forming the emitter contacts on InGaP top cells, (iii) etching III-V layers for forming mesas, (iv) depositing anti-reflection films, (v) etching Si emitters for isolation, and (vi) forming the base contacts on the bottom of Si cells. The schematic cross section of 3J cells and the entire process sequence are shown in Fig. 3. An image of surface of the III-V epi layer after the selective etching of GaAs substrates is also shown in this figure. The entire epi layer was firmly attached on the Si bottom cell, which suggests that the bonding interface has an enough tolerance against the semiconductor device process.

The $I - V$ characteristics of a 3J cell with a 5-mm-by-5-mm III-V mesa under the solar irradiance (AM1.5G/one sun) are shown in Fig. 4(a). The apparent short-circuit current J_{SC} , open-circuit voltage, conversion efficiency, fill factor, and series resistance were $10.7 \text{ mA}/\text{cm}^2$, 2.92 V , 25.5% , 81.5% , and $17.6 \text{ }\Omega\text{cm}^2$, respectively. The III-V mesa in the 3J cell was surrounded by a Si ledge with an extension of $20 \text{ }\mu\text{m}$, which was likely to contribute to the $I - V$ characteristics. The intrinsic J_{SC} and efficiency of 3J cells were rudely estimated to be $11.3 \text{ mA}/\text{cm}^2$ and $\sim 26\%$, respectively, by subtracting the contribution of the Si ledge and that of the shadow loss

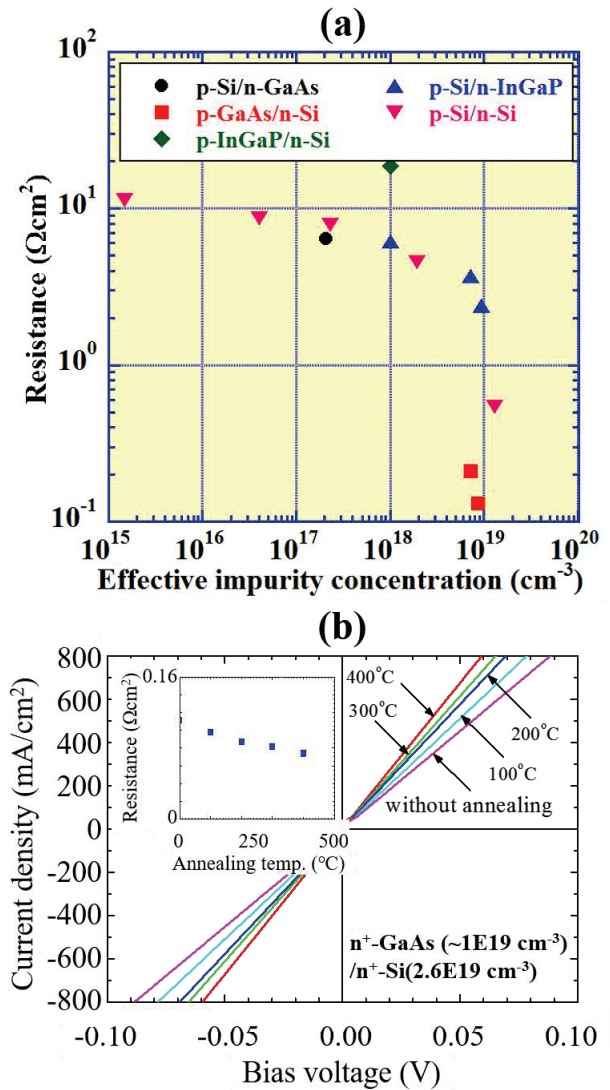


Fig. 2. (a) Resistances across bonding interfaces of pn junctions with different impurity concentrations. Lower resistances are observed in interfaces of bonding layers with higher doping concentrations. (b) $I - V$ characteristics of $n\text{-GaAs}/n\text{-Si}$ junctions. Lower resistances are obtained by annealing at higher temperatures as the inset shows.

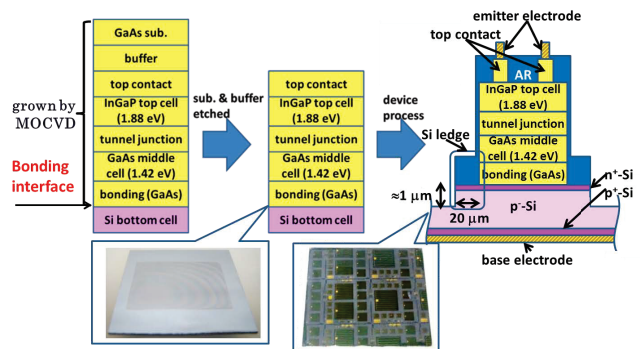


Fig. 3. The process sequence for fabricating InGaP/GaAs/Si triple-junction cells and their schematic cross section.

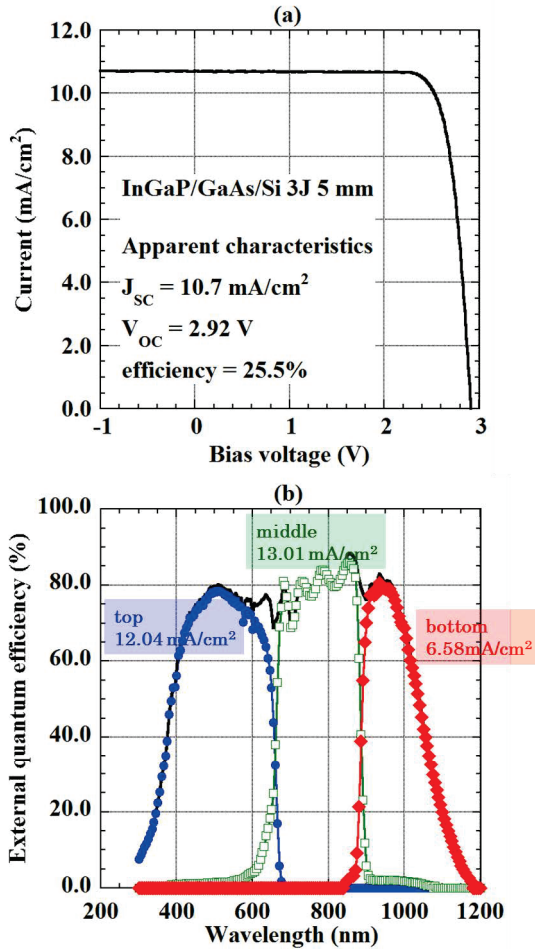


Fig. 4. (a) The $I - V$ characteristics of a 5-mm-by-5-mm InGaP/GaAs/Si triple-junction cell under the solar irradiance. (b) The external quantum efficiency spectra of the InGaP/GaAs/Si triple-junction cell.

due to emitter contacts on the top cells. Figure 4(b) shows the spectra of the external quantum efficiency of the 3J cell. The currents generated under the AM1.5G/one sun condition were estimated to be 12.04, 13.01, and 6.58 mA/cm^2 for the top, middle, and bottom cells, respectively. The current generated in the bottom cell was smaller than J_{SC} of the 3J cell although those in the top and middle cells were close to J_{SC} . The structure of the bottom cell should be revised for suppressing the current mismatch among sub cells and improving the performance of the 3J cell. Another part to be improved is the resistance across the bonding interface, which was recently found to be larger than that in heavily-doped GaAs substrate/Si substrate junctions.

IV. CONCLUSION

The surface-activated bonding (SAB) technologies were applied for forming GaAs/Si heterojunctions as well as Si/Si and GaAs/GaAs homojunctions. Lower resistances across the bonding interfaces were obtained by using bonding layers with higher doping concentrations and annealing the interfaces. The change in the resistance was discussed in conjecture

with the narrower potential barriers at the interface and the lower densities of the interface states due to the annealing, respectively. InGaP/GaAs/Si hybrid triple-junction cells were successfully fabricated by using the SAB technologies and subsequent device process sequences, which indicates that the SAB technologies are practically applicable for fabricating novel functional devices that cannot be made by using the conventional epitaxial growth technologies.

ACKNOWLEDGMENT

Heterostructures for InGaP/GaAs 2J cells were prepared by Sharp Corporation. This work was supported by the “Research and Development of ultra-high efficiency and low-cost III-V compound semiconductor solar cell modules (High efficiency and low-cost III-V/Si tandem)” project of New Energy and Industrial Technology Development Organization (NEDO) and “Creative research for clean energy generation using solar energy” program of Japan Science and Technology Agency (JST).

REFERENCES

- [1] http://www.nrel.gov/ncpv/images/efficiency_chart.jpg.
- [2] F. Dimroth, et al. Prog. Photovolt: Res. Appl. **22** (2014) 277.
- [3] O. Moutanabbir and U. Gösele, Annu. Rev. Mater. Res. **40** 469 (2010).
- [4] H. Takagi, K. Kikuchi, R. Maeda, T. R. Chung, and T. Suga, Appl. Phys. Lett. **68** 2222 (1996).
- [5] H. Takagi, R. Maeda, N. Hosoda, and T. Suga, Jpn. J. Appl. Phys. **38** 1589 (1999).
- [6] M. M. R. Howlader, T. Watanabe, and T. Suga, J. Vac. Sci. Technol. B **19** 2114 (2001).
- [7] N. Shigekawa, L. Chai, M. Morimoto, J. Liang, R. Onitsuka, T. Agui, H. Juso, and T. Takamoto, Proc. 40th IEEE Photovoltaic Specialists Conference, pp. 534-537 (2014).
- [8] N. Shigekawa, J. Liang, R. Onitsuka, T. Agui, H. Juso, and T. Takamoto, J. Appl. Phys. **54**, 08KE03 (2015).
- [9] J. Liang, S. Nishida, M. Morimoto, and N. Shigekawa, Elec. Lett. **49**, 830 (2013).
- [10] J. Liang, L. Chai, S. Nishida, M. Morimoto, and N. Shigekawa, Jpn. J. Appl. Phys. **54**, 030211 (2015).
- [11] M. Morimoto, J. Liang, S. Nishida and N. Shigekawa, Jpn. J. Appl. Phys. **54**, 030212 (2015).
- [12] L. Chai, J. Liang, and N. Shigekawa, Jpn. J. Appl. Phys. **55** 068002 (2016).
- [13] J. Robertson and B. Falabretti, J. Appl. Phys. **100** 014111 (2006)